

Low-aspect-ratio RFP plasma properties in two characteristic regimes in RELAX

Sadao Masamune, A. Sanpei, K. Oki, D. Fukabori, K. Deguchi, S. Nakaki, H. Himura, R. Ikezoe¹⁾, T. Onchi²⁾, N. Nishino³⁾, R. Paccagnella⁴⁾, A. Ejiri⁵⁾, T. Akiyama⁶⁾, K. Kawahata⁶⁾, J.K. Anderson⁷⁾, D.J. Den Hartog⁷⁾, H. Koguchi⁸⁾

Kyoto Institute of technology, Kyoto, Japan, ¹⁾University of Tsukuba, Tsukuba, Japan, ²⁾University of Saskatchewan, Saskatoon, Canada, ³⁾Hiroshima University, Higashi-Hiroshima, Japan, ⁴⁾Consorzio RFX, Padova, Italy, ⁵⁾University of Tokyo, Kashiwa, Japan, ⁶⁾National Institute for Fusion Science, Toki, Japan, ⁷⁾University of Wisconsin, Madison, USA, ⁸⁾National Institute for Advanced Industrial Science and Technology (AIST), Tsukuba, Japan

1. Introduction

The reversed field pinch (RFP) is one of the magnetic confinement concepts for high-beta plasmas. Recent progress in understanding and controlling MHD instabilities in the RFP configuration has led to improved plasma confinement comparable to the tokamak L mode scaling. One of the advantages of the RFP configuration is that it has a potential to confine reactor-relevant high beta plasmas with much weaker external toroidal field than in tokamaks, which may allow us to use normal conductors for the toroidal field in RFP fusion reactors.

One of the requirements for high-performance RFP reactor concepts is to establish scenarios for toroidal current drive other than conventional Ohmic current drive. One of the possibilities is to lower the aspect ratio $A (=R/a$, where R (a) is the major (minor) radius); A theory predicts that the pressure-driven bootstrap current would become sizable by lowering A below 2 with rather high beta values. Another interesting feature of the low- A RFP configuration is the q profile. As the aspect ratio is lowered, more space would become available in the core region without major resonant surface if we could choose an adequate value of the on-axis safety factor (q) value q_0 . It then would become easier for the core resonant tearing mode to grow without interacting with the neighboring mode. This characteristic would be beneficial to good confinement of RFP with quasi-single helicity (QSH) state where the helically deformed core is embedded in the outer axisymmetric flux surfaces.

2. RELAX machine

We have constructed a low- A RFP machine RELAX (REversed field pinch of Low-Aspect-ratio eXperiment) with $R=0.51\text{m}$ and $a=0.25\text{m}$. It uses a 4-mm thick SS vacuum vessel which acts as a resistive wall; No conducting wall or shell has been attached. The vessel has a poloidal gap for inductive Ohmic current drive, and no toroidal gap. Our recent

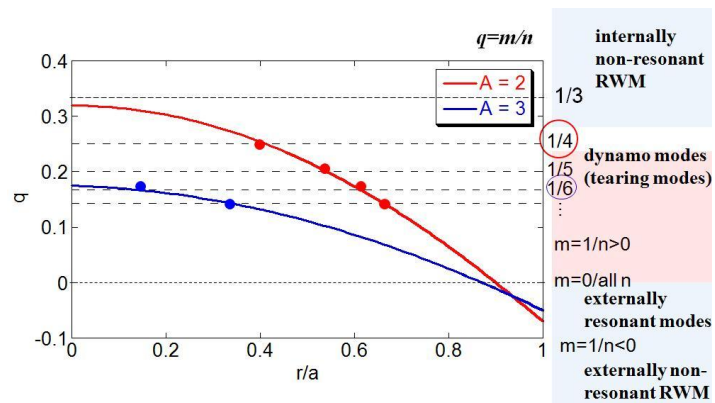


Fig.1 Typical q profiles for $A=3$ and 2 RFP configurations.

analysis has shown that if we could achieve poloidal beta value around 30%, the bootstrap fraction of 25-30% would be expected. This corresponds to the following plasma parameters for RELAX plasmas: central electron temperature T_{e0} of ~ 300 eV with central electron (and ion) density n_e (n_i) of $\sim 3 \times 10^{19} \text{ m}^{-3}$ at plasma current I_p of 100kA. The major objectives of RELAX include realizing improved confinement and experimental verification of the bootstrap current by achieving beta values around 30%. During the process of discharge optimization, we have found two operational regions which have a potential confinement improvement; One is the helically deformed plasma or QSH state, and the other is the extremely deep reversal plasmas characterized by broad magnetic fluctuation spectrum with lowered amplitudes. We will describe features of low-A RFP plasmas in these two discharge regimes. Figure 1 compares the q profiles for $A=3$ and $A=2$ cases, showing that in the latter case the innermost resonant surface could be located at $r/a \sim 0/4$ if we could avoid the on-axis resonance of $q_0=1/3=0.33$. And at the same time, it can be expected that the toroidal mode spectrum of the $m=1$ mode would shift to lower n side as the aspect ratio is lowered.

3. Experimental (Θ, F) regions

The RFP discharge regime is often characterized by the pinch parameter $\Theta = B_{\theta a} / \langle B_{\phi} \rangle$, defined as the ratio of the edge poloidal field to the average toroidal field, a measure of plasma current for a given value of toroidal magnetic flux, and F , the fields reversal parameter defined by $F = B_{\phi a} / \langle B_{\phi} \rangle$, a measure of the degree of toroidal field reversal for a given value of toroidal magnetic flux. Figure 2 shows the discharge

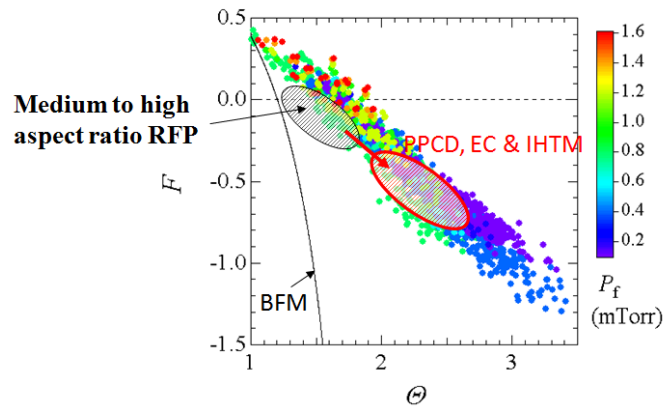


Fig.2 Discharge regions of RELAX plasmas in (Θ, F) space. Typical regions for medium- to high-aspect-ratio RFP plasmas are also shown.

regimes attained in RELAX in (Θ, F) space. In standard RFP plasmas with medium- to high-A, Θ lies in the range $1.4 < \Theta < 2$, and F , $-0.4 < F < 0$. For the improved operation mode such as improved high Θ mode (IHTM), enhanced confinement mode (EC), and pulsed parallel current drive (PPCD), Θ tends to be higher with deeper F . In RELAX, the operational regimes are extended to higher Θ and deeper F regions to $\Theta \sim 3.5$ with $F \sim -1.5$. Θ and F values keep some (off-set) linear relations over the whole discharge regimes, which indicates that the magnetic field profiles have some constraints, meaning self-organized magnetic field profiles over the discharge regions. We have identified two characteristic regions: shallow-reversal regions where F values lie slightly negative close to 0 and extremely deep reversal regions where the edge toroidal field reverses much more than in conventional RFPs. Both of these two regions have a potential confinement improvement, as will be discussed in the following sections.

4. Soft-X ray imaging of helix

We have developed soft-X ray diagnostics for detailed study of magnetic structures mainly in QSH plasmas. Following the visible-light high-speed camera diagnostic which allowed us to observe simple helix structure at QSH phase, we have developed a SXR pin-hole camera for tangential imaging of the plasma column. When we use the pin-hole camera with a fluorescent plate with short (of the order of micro second) decay time in combination with a high-speed camera, we can obtain the time evolution of SXR images. When we further apply subtracting technique to two of the framing pictures taken with $10 \mu\text{s}$ time separation, we have obtained a fluctuating component of SXR image by minimizing the effect of slowly varying background SXR emissivity. Figure 3 shows an example of the difference in two consecutive images showing a simple helix in the SXR emission. The structure corresponds to the change in SXR emissivity probably due to rotation of the helical hot region in $10 \mu\text{s}$. The simple helix resembles the structure of the visible-light image. We can conclude that a simple helical SXR structure which has higher SXR emissivity than the background rotates in the QSH phase. Comparison of the phase relationship between the SXR helix structure and edge magnetic fluctuation has revealed that the SXR helix corresponds to the O-point of the magnetic island associated with the dominant mode. In extremely deep reversal discharges, magnetic fluctuation level decreased and SXR emission increased, indicating improved plasma performance in this regime. Details of the discharge features in this region are described in ref. [4].

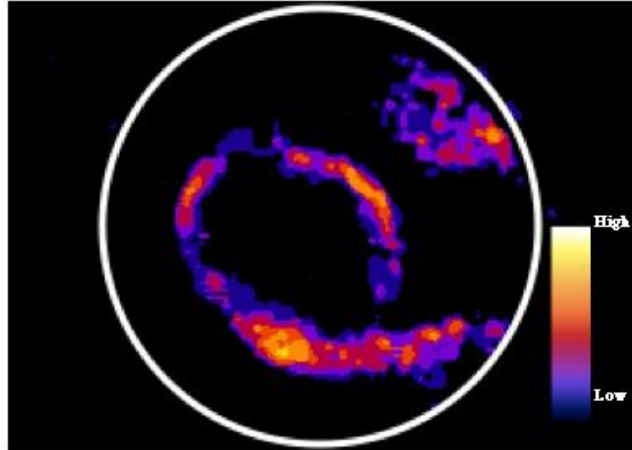


Fig.3 Simple filament structure of SXR emissivity observed in a tangential image in RELAX.

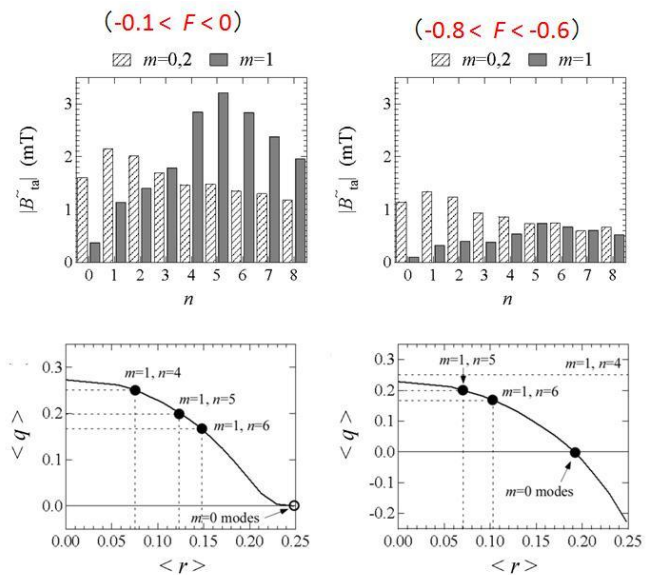


Fig.4 Toroidal mode spectra of $m=1$ and $m=0$ modes with q profiles in shallow- and deep-reversal RFP plasmas.

5. Mode spectra of edge magnetic fluctuations

In Fig. 4, we have compared the q profiles and toroidal mode spectra of the $m=0$ and $m=1$ modes for the RFP plasmas in these shallow- and deep-reversal regions. The magnetic fluctuation amplitudes concentrate to 2-3 dominant modes in shallow-reversal case, while the spectrum

becomes broad with lower amplitudes in deep-reversal case. The difference may be attributable to the difference in q profile, where magnetic shear is stringer in the outer region in deep-reversal case.

6. 3-D MHD simulation

The dependence of the magnetic fluctuation mode spectrum on the equilibrium RFP profiles have been studied with 3-D MHD simulation. The numerical code was used for Spherical Tokamaks and Large Helical Device for the study of MHD behavior with great success. This code has been modified for the $A=2$ RELAX plasma configuration, and initial equilibrium profiles were provided by the reconstruction code RELAXFit. The initial results have shown that when the field reversal is shallow, the RFP tends to relax to a single helical state where the core resonant $m=1/n=4$ mode grows to a significant amplitude, and the QSH state persists. On the other hand, when the initial equilibrium has deep reversal profile, the magnetic mode spectrum becomes broad with lower amplitudes. Thus, the major features of the experimental results on the dependence of magnetic fluctuation mode spectra on the equilibrium field profiles can be reproduced qualitatively. Figure 5 shows the dependence on the Prandtl number $P=\nu/\mu$ of the toroidal mode spectrum of the $m=1$ modes after relaxation, where Prandtl number $P=\nu/\mu$, the ratio of viscosity to resistivity. As P increases, the fluctuation power concentrates to the single dominant $m=1/n=4$ mode in the case of $A=2$ RFP configuration. The trend is similar to the previous 3D MHD simulations using cylindrical approximation for the RFP equilibrium configuration[6].

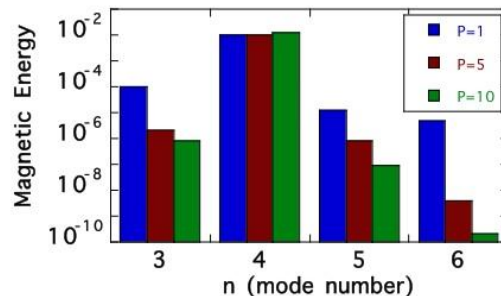


Fig.5 Dependence of toroidal mode spectrum on Prandtl number $P=\nu/\mu$.

7. Summary

$A=2$ RFP plasmas have been obtained in a low- A machine RELAX. Two characteristic discharge regions have been found, both of which have a potential confinement improvement. Further efforts are in progress to realize high-beta plasmas where sizable bootstrap current is expected.

Acknowledgment

This work has been supported by a grant in aid for scientific research from MEXT (22360390) and by a NIFS collaboration program (NIFS10KOAP024).

References

- [1] P. Martin et al., Nucl. Fusion 49, 104019 (2009).
- [2] B.E. Chapman et al., Nucl. Fusion 49, 104020 (2009).
- [3] K. Oki et al., J. Phys. Soc. Jpn. 77, 075005 (2008).
- [4] R. Ikezoe et al., Plasma Phys. Control Fusion 53, 025003 (2011).
- [5] T. Onchi et al., accepted for publication in J. Phys. Soc. Jpn. 80 (2011).
- [6] S. Cappello S and D. F. Escande, Phys. Rev. Lett. 85, 3838 (2000).